SLAC PUB 4583
SLAC TPC 4
November 1987
(N)

Degradation of NIT beam due to beam windows

G. Zaparac, E. Bloom, H. Band, R. Prepost, K. Moffeit, M. Donald
Stanford Linear Accelerator Center
P.O. Box 4349
Stanford, California 94309

I. Emittance growth

The increase in emittance of the NIT beam due to multiple scattering from windows at magnet B11 and at the polarimeter detector was studied using TRANSPORT. Runs were made for both a 13.5 GeV SLC beam (TRAN NIT13 on account GEORDIE) and an 8 GeV NPI beam (TRAN NPI8). The momentum dispersion was taken to be zero for both studies. Nominal beam parameters assumed at sector 30 were $\sigma_x = \sigma_y = 0.237$ mm with $\sigma_{x'} = \sigma_{y'} = 0.00481$ mrad at 13.5 GeV, and $\sigma_x = \sigma_y = 0.973$ mm with $\sigma_{x'} = \sigma_{y'} = 0.0197$ mrad at 8 GeV. These values correspond to SLC and NPI emittances of 0.0011 mm-mrad and 0.0192 mm-mrad, respectively, or to invariant SLC and NPI emittances of $3 \cdot 10^{-5}$ m-rad and $3 \cdot 10^{-4}$ m-rad. The effect of the windows was simulated by adding the RMS multiple scattering angle to the beam divergence in both the x and y planes at the z-position of the windows.

The beam windows for the polarimeter detector were taken to be two 0.0013 cm Fe windows separated by 20 cm of He. This represents 0.00148 radiation lengths and an RMS projected multiple scattering angle of 28 μrad at 13.5 GeV or 47 μrad at 8 GeV. There is a pair of windows at each end of the septum magnet B11. These windows separate the NIT vacuum, the He filled beam pipe inside B11 (300 cm), and the PEP vacuum. Both pairs of windows are separated by about 10 cm of air. Each pair is estimated to represent at least 0.0028 radiation lengths with a scattering angle of 40 μrad at 13.5 GeV and 61 μrad at 8 GeV.

We have also considered a scenario with only two windows downstream of B11 and with only a single window downstream of B11. For the case of two windows, the beam pipe inside B11 is at the NIT vacuum. These windows then represent 0.0024 radiation lengths and a scattering angle of 36 μrad for 13.5 GeV and 61 μrad for 8 GeV. We must have at least one window to separate the PEP and NIT vacuums. A single 0.0013 cm Fe window represents 0.00072 radiation lengths and a scattering angle of 18 μrad at 13.5 GeV and 30 μrad at 8 GeV.

Table 1 shows the TRANSPORT results for emittances calculated in the x and y

Work supported by the Department of Energy under contract DE-AC03-76SF00515.

(Submitted for Publication)

planes immediately after B11. The three different cases of windows at B11 are shown at both energies, with and without the polarimeter windows. For the present case with four windows at B11, the emittance increases by about 20% after the polarimeter windows are introduced. The emittance decreases by a factor of three if the four windows at B11 are replaced by a single 0.0013 Fe window.

The emittance growth has also been studied by the Polarization Group using TRANSPORT. An emittance of 0.0035 mm-mrad at 14.5 GeV is assumed here; this is probably closer to the emittance of the SLC beam delivered next year. The results for three polarimeter materials are shown in Table 2. Both studies found agreement between TRANSPORT and TURTLE for the dimensions of the phase space ellipse.

Using TRANSPORT, we have attempted to match the Twiss parameters of the injected beam to the PEP acceptance at kicker magnet K2. We have the freedom to adjust three quadrupole strings in the transport line. A match is considered successful if $\beta_x = 20m$ and $\alpha_x = 0$. The match succeeded for the case of no windows or for a single 0.0013 cm Fe window at B11 (Figures 1-4; the inner contour represents 2σ, the outer 3σ). We were not able to match the Twiss parameters after the detector windows were added (Figures 5-6). Any adjustment of the Twiss parameters with four windows at B11 is impossible because the size of the phase space ellipse is dominated by the multiple scattering downstream of all of the quadrupole magnets (Figures 7-8). In Figures 9-14 we show the injection of the NPI beam. The phase space of the PEP emittance for electrons during previous running (0.0075 mm-mrad) is shown in Figures 15-16.

The TPC group recommends putting PR9 and PR10 in vacuum for two reasons: 1) the emittance of the beam entering PEP is reduced by a factor of 2 to 3 in the NIT line if the detector windows are present, and by a factor of 3 to 4 in the SIT line where no detector windows are present, and, 2) any adjustment of the Twiss parameters upstream of the septum magnet is meaningless if the four profile monitor windows are not removed.

II. Spray into BPMs

A small fraction of the electrons will have a large momentum dispersion after the polarimeter windows. Any electrons off momentum by more than 6.7% are deflected outside of the beam pipe (3.8 cm radius) by the dipole magnet B3 before they reach the next x-focussing quadrupole Q2 (see Figure 17). In this study it is assumed that any particles outside of the beam pipe at Q2 will not reach the BPMs because they are blocked by the magnet. This implies an energy cutoff at 12.6 GeV for a 13.5 GeV beam. To estimate the fraction of electrons with a large momentum dispersion, EGS was run to simulate 100,000 electrons impinging upon a slab of Fe with a thickness equivalent to the radiation lengths of the polarimeter windows (0.0026 cm). The fraction of electrons with energies between 12.6 and 13.4 GeV after exiting the slab is 0.0045.

TURTLE was run with 10,000 rays and all of the magnet apertures to estimate the fraction of the beam that could strike the BPMs. Quadrupole apertures were approximated by a circular slit with a radius equal to the half gap (1 inch). Dipole magnet apertures were represented as a slit separated by the gap between poles (1 inch, with the exception of BVA, which has a 2 inch gap). Dipole B3 is given a rectangular aperture 3 inches wide and 1 inch high. The emittance at the start of the deck was 0.004 mm-mrad.

Each BPM was bounded in z by two circular slits with the same radius as the beam pipe (Figure 17). Any electrons blocked by either of these slits could strike the BPMs. The product of the fraction of electrons that have a high dispersion (estimated by EGS) and the fraction of high dispersion electrons that are blocked by the slits (as determined by TURTLE) is taken as the fraction f of electrons that could strike the BPMs.

A momentum dispersion of 6.7% was added to the beam at the position of the detector windows. Only BPMs 1 and 3 were affected (Table 3). BPM3 is the most vulnerable, with $f = 3 \cdot 10^{-4}$. In Table 4 f is checked for dispersions of 3.7% and 7.4%. For the purpose of this rough estimate, the answer appears reasonably insensitive.

TURTLE was used to scatter plot the ray position at BPMs 1, 2, 3, and 4 (Figures 18-21). The straight lines represent a distance of 3.8 cm from the beam axis in x (the beam pipe radius) and 5 mm from the beam axis in y. The BPM strips have been oriented at 45° in anticipation of a large dispersion; a beam with $\sigma_x = 5.9$ mm is 4σ from the closest edge of the strip. The effect of spray in the horizontal plane on BPM performance will be studied during injection tests.

The spray near the BPMs has also been investigated by the Polarization Group using TURTLE and EGS. In this study, 10,000 rays initiated by TURTLE were run through an EGS simulation of the detector windows before being read back into TURTLE and transported to the end of the NIT line. This study concludes that BPMs 1, 2, and 4 are not vulnerable to the increased dispersion from the windows, but that BPM 3 is vulnerable to the fraction $3 \cdot 10^{-4}$, in good agreement with the other study.

III. Summary and Conclusions

We have estimated that the windows for the polarimeter detector increase the beam emittance by about 20% if we run with all four B11 windows in place. The four B11 window increase the emittance by a factor of 3 over the scenario where the PEP and NIT/SIT vacuums are separated by a single 1/2 mil stainless steel window. The increase in dispersion due to multiple scattering at the detector has been estimated by EGS and TURTLE to cause 0.03% of the beam to spread beyond the beam pipe radius near BPM 3. Additional shielding of the BPMs (besides the magnets) may be required. The need for such shielding will be reviewed after data is obtained.

The emittance at the kicker magnet is completely dominated by the multiple scattering from the four B11 windows. The TPC group recommends putting profile monitors PR9 and PR10 in vacuum before PEP HEP this June. This eliminates the four B11 windows and reduces the emittance by a factor of 3. It also allows, at least in the SIT line, the ability to adjust the Twiss parameters of the injected beam. Once PR9 and PR10 are in vacuum, the effect of the polarimeter windows is an increase of the beam emittance by a factor of 2. We do not anticipate that this degradation will cause a problem.

In order to address the possible need to shield the BPMs, and to study the effect of emittance growth on the injection efficiency, the Polarization and TPC groups have agreed upon the following installation schedule. PEP would debug and run with the present vacuum pipe at the polarimeter detector position. The polarimeter windows would be installed on the existing flanges in a one day (or less) access and the polarization tests would proceed. If necessary the vacuum pipe could be easily reinstalled for further PEP running. PEP would at some time inject with the polarimeter windows in place to study injection efficiency and possible backgrounds.

TABLE 1

Emittances from TRANSPORT using 0.5 mil Fe detector windows separated by 20 cm of He. Emittances are in mm-mrad and are taken at kicker magnet K2. Nominal emittances in both transverse planes are 0.0011 mm-mrad for SLC (13.5 GeV) and 0.0192 mm-mrad for NPI (8 GeV).

	ϵ_x (SLC)	ϵ_y (SLC)	ϵ_x (NPI)	ϵ_y (NPI)
No windows	0.0012	0.0011	0.0197	0.0200
Detector windows only	0.0051	0.0042	0.0399	0.0340
Four B11 windows	0.0099	0.0076	0.0639	0.0463
Four B11 windows and detector windows	0.0122	0.0101	0.0742	0.0556
Two windows downstream of B11	0.0058	0.0036	0.0445	0.0311
Two windows at B11 and detector windows	0.0077	0.0071	0.0558	0.0438
One 0.5 mil Fe window downstream of B11	0.0031	0.0021	0.0276	0.0232
One 0.5 mil Fe window and detector windows	0.0060	0.0051	0.0439	0.0364
Former PEP electron beam at 13.5 GeV with $\epsilon_x = \epsilon_y = 0.0075$	0.0212	0.0185		

TABLE 2

TRANSPORT STUDIES

Radiation Lengths and θ_{plane}^{rms} for the different cases

Case	Radiation Lengths	θ_{plane}^{rms}(by formula)	θ_{plane}^{rms}(by EGS4)
A.	3.5×10^{-3}	41.7μrad	47.0μrad
B.	0.76×10^{-3}	17.4μrad	21.4μrad
C.	1.55×10^{-3}	26.0μrad	28.5μrad
D.	1.21×10^{-3}	25.1μrad	

Beam after B11 ignoring end of NIT windows

	σ_x(mm)	$\sigma_{x'}$(mr)	σ_y(mm)	$\sigma_{y'}$(mr)	r_{21}	r_{43}	ϵ_x(mm-mr)	ϵ_y(mm-mr)
Nominal	0.279	0.016	0.168	0.022	0.484	-0.098	0.0039	0.0037
A. 5mil Al(2)+20cm Air	0.284	0.054	0.272	0.065	-0.027	0.720	0.015	0.012
B. 5mil Be(2)+20cm He	0.280	0.028	0.194	0.036	0.202	0.343	0.0077	0.0066
C. 0.5mil SS(2)+20cm He	0.281	0.035	0.212	0.043	0.121	0.488	0.0098	0.0080

Beam after B11 with windows before and after B11

	σ_x(mm)	$\sigma_{x'}$(mr)	σ_y(mm)	$\sigma_{y'}$(mr)	r_{21}	r_{43}	ϵ_x(mm-mr)	ϵ_y(mm-mr)
Nominal	0.301	0.054	0.200	0.056	0.377	0.321	0.015	0.0106
A. 5mil Al(2)+20cm Air	0.304	0.074	0.293	0.083	0.155	0.688	0.0220	0.0176
C. 0.5mil SS(2)+20cm He	0.300	0.062	0.238	0.067	0.274	0.526	0.0179	0.0136
D. 2mil Al(2)+20cm He	0.301	0.060	0.230	0.065	0.294	0.492	0.0173	0.0131

TABLE 3 (*see Figure 17*)

BPM	N_1	N_2	N_3	$f = 0.0045(N_1 - N_3)/N_0$
1	4934	4934	4924	$4.5 \cdot 10^{-6}$
2	3233	3233	3233	0
3	3233	2781	2552	$3.1 \cdot 10^{-4}$
4	1279	1279	1279	0
5	551	551	551	0
6	551	551	551	0

TABLE 4

To check the sensitivity of f (defined in TABLE 2) to $\delta p/p$, TURTLE was run with $\delta p/p = 3.7\%$ and $\delta p/p = 7.4\%$.

$\delta p/p$	f	$(N_1 - N_3)/N_3$
3.7%	$4.8 \cdot 10^{-4}$	0.195
6.7%	$3.1 \cdot 10^{-4}$	0.211
7.4%	$2.8 \cdot 10^{-4}$	0.209

Figure 1: 13.5 GeV beam with no windows

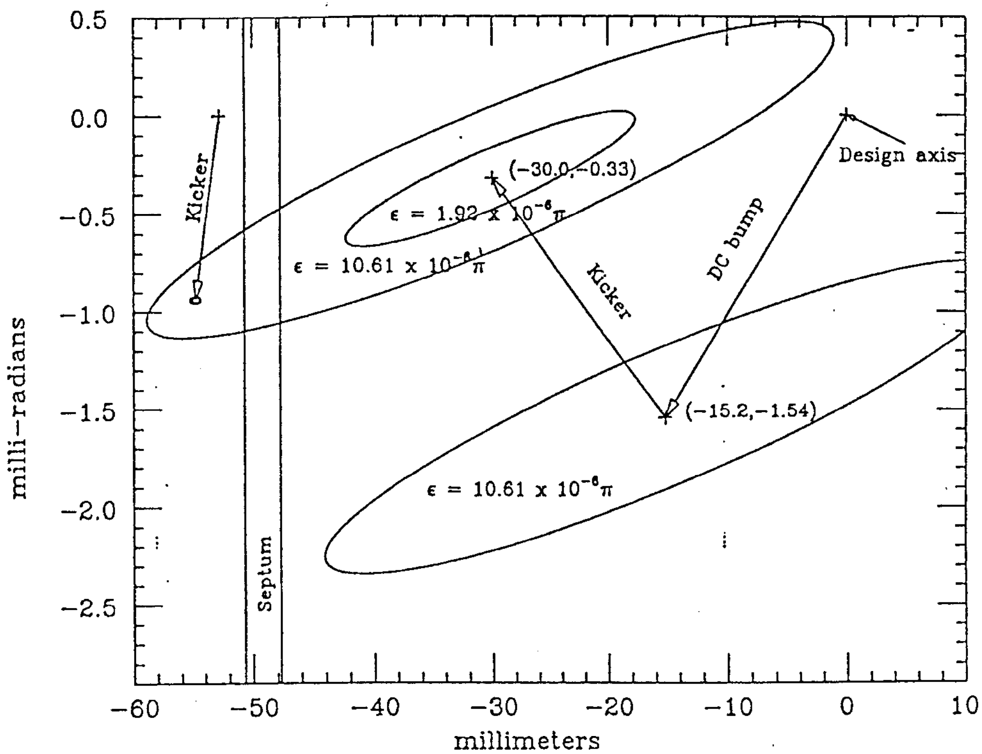

Horizontal phase space at exit of kicker magnet K2, showing injection for colliding beams.

Figure 2: 13.5 GeV beam with no windows

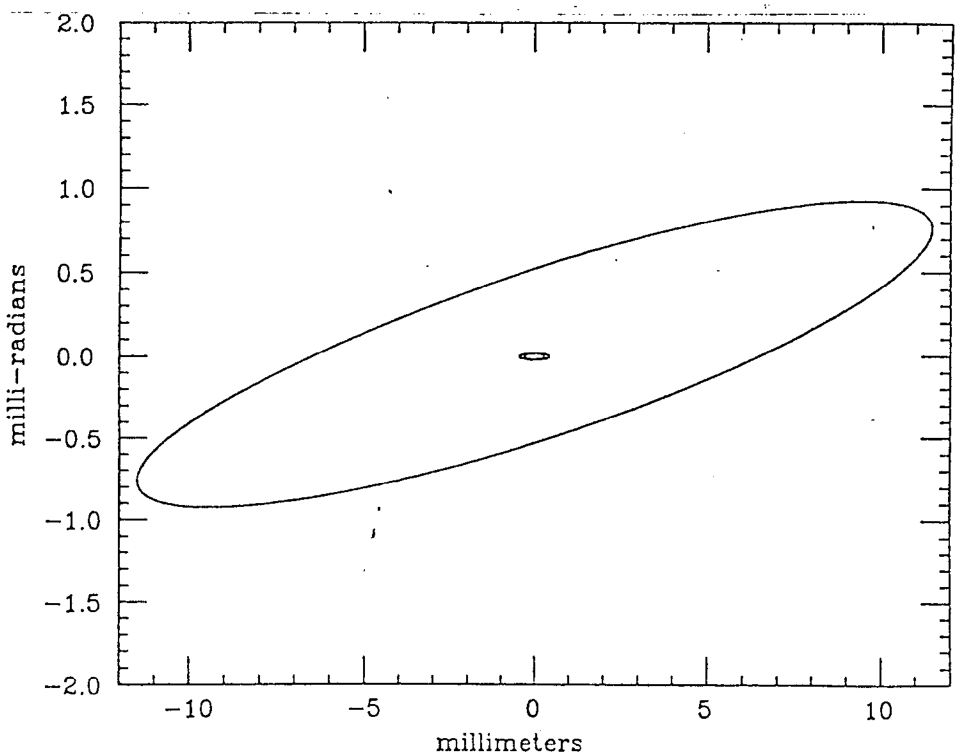

Vertical phase space at exit of kicker magnet K2, showing injection for colliding beams.

Figure 3: 13.5 GeV beam with single
0.5 mil Fe window

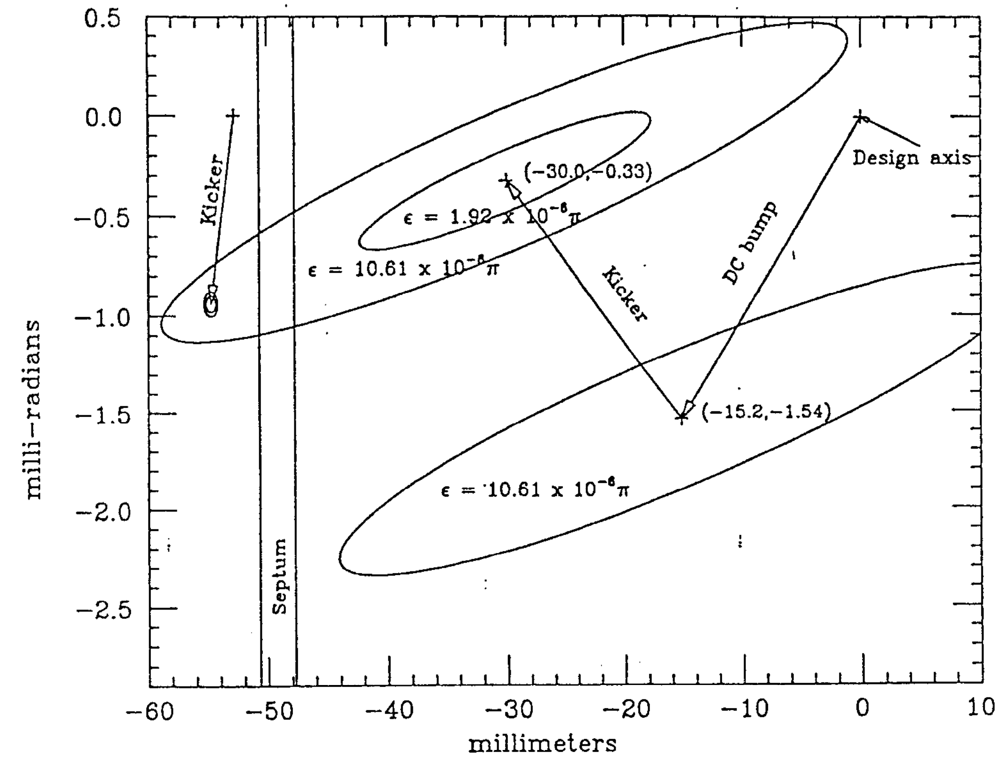

Horizontal phase space at exit of
kicker magnet K2, showing injection
for colliding beams.

Figure 4: 13.5 GeV beam with single
0.5 mil Fe window at B11

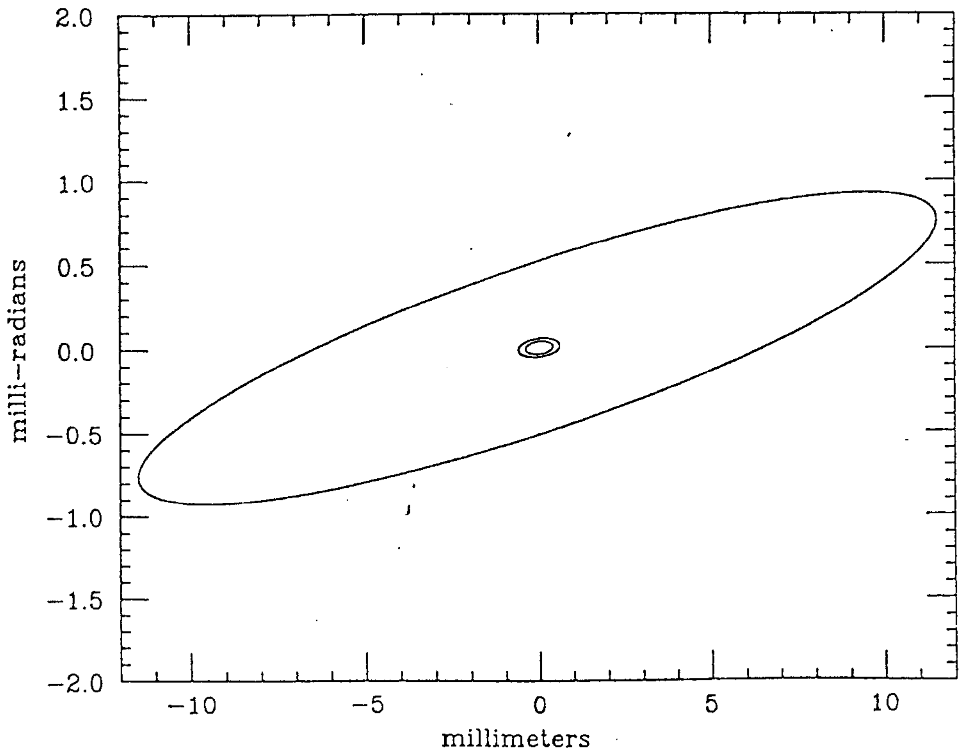

Vertical phase space at exit of
kicker magnet K2, showing injection
for colliding beams.

Figure 5: 13.5 GeV beam with detector windows and single 0.5 mil Fe window at B11

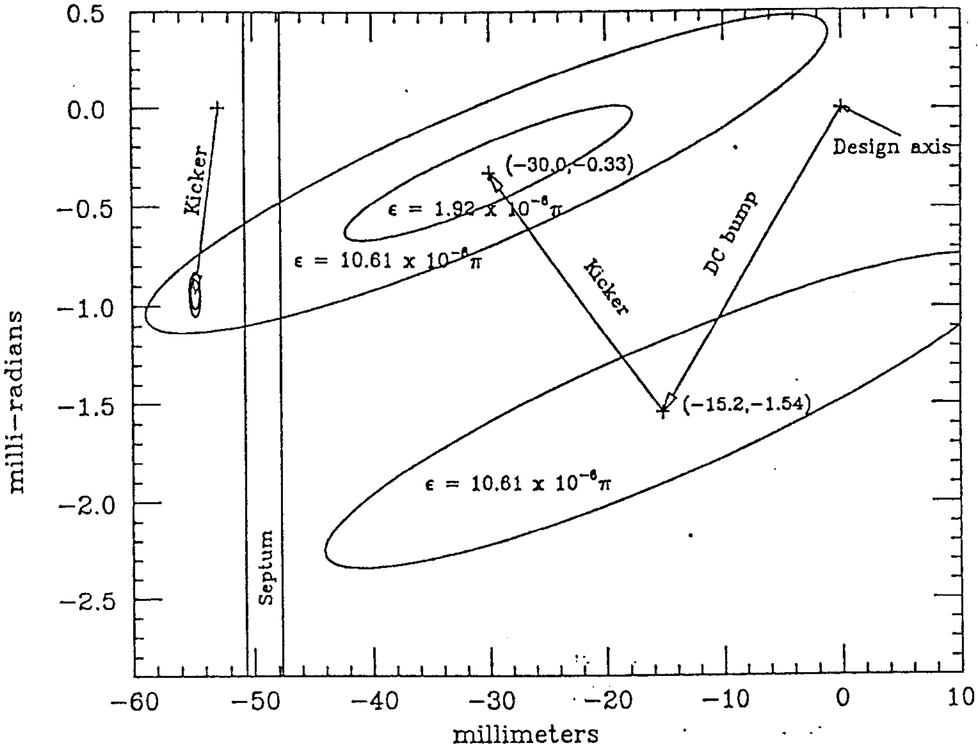

Horizontal phase space at exit of kicker magnet K2, showing injection for colliding beams.

Figure 6: 13.5 GeV beam with detector windows and single 0.5 mil Fe window at B11

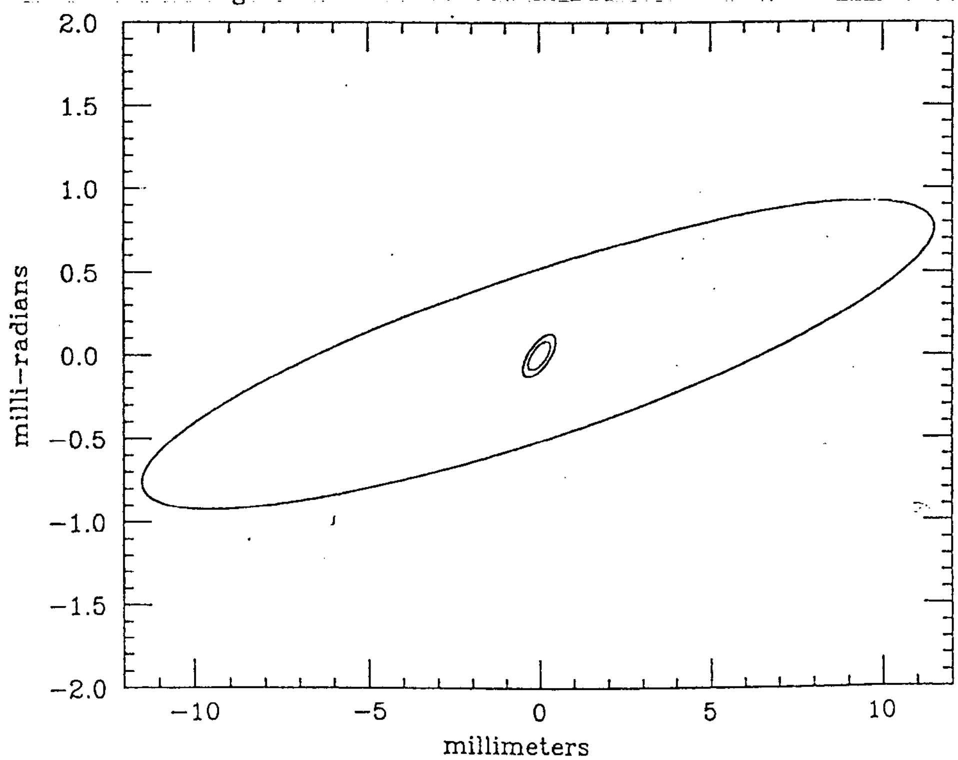

Vertical phase space at exit of kicker magnet K2, showing injection for colliding beams.

Figure 7: 13.5 GeV beam 4 B11 windows

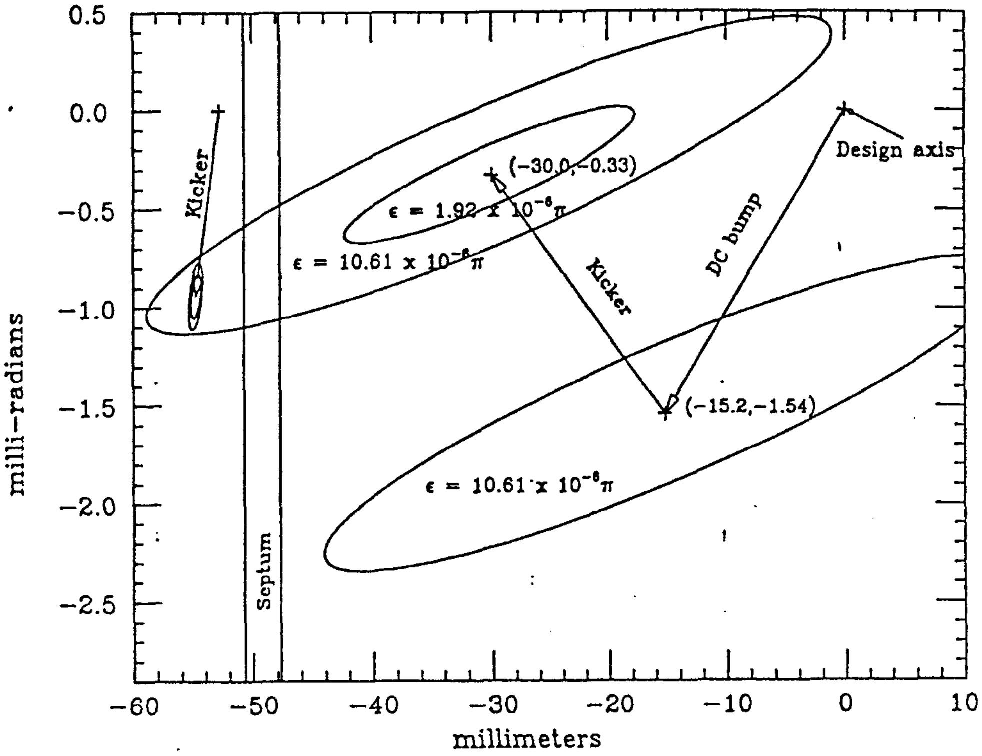

Horizontal phase space at exit of kicker magnet K2, showing injection for colliding beams.

Figure 8: 13.5 GeV beam with 4 B11 windows

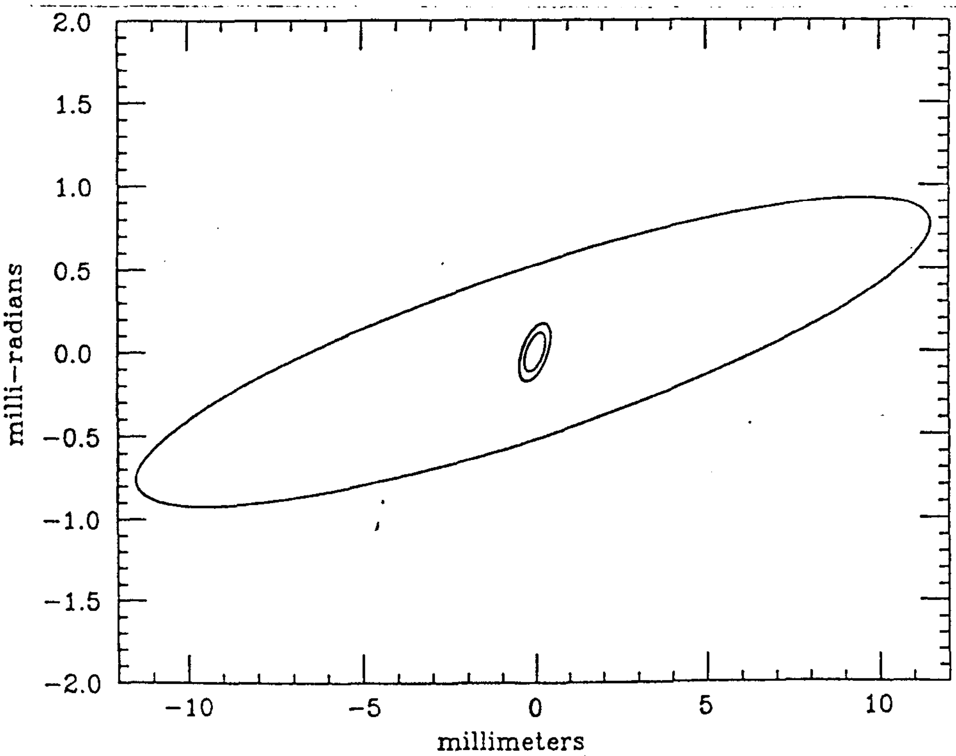

Vertical phase space at exit of kicker magnet K2, showing injection for colliding beams.

Figure 9: 8 GeV NPI beam with single 0.5 mil B11 window

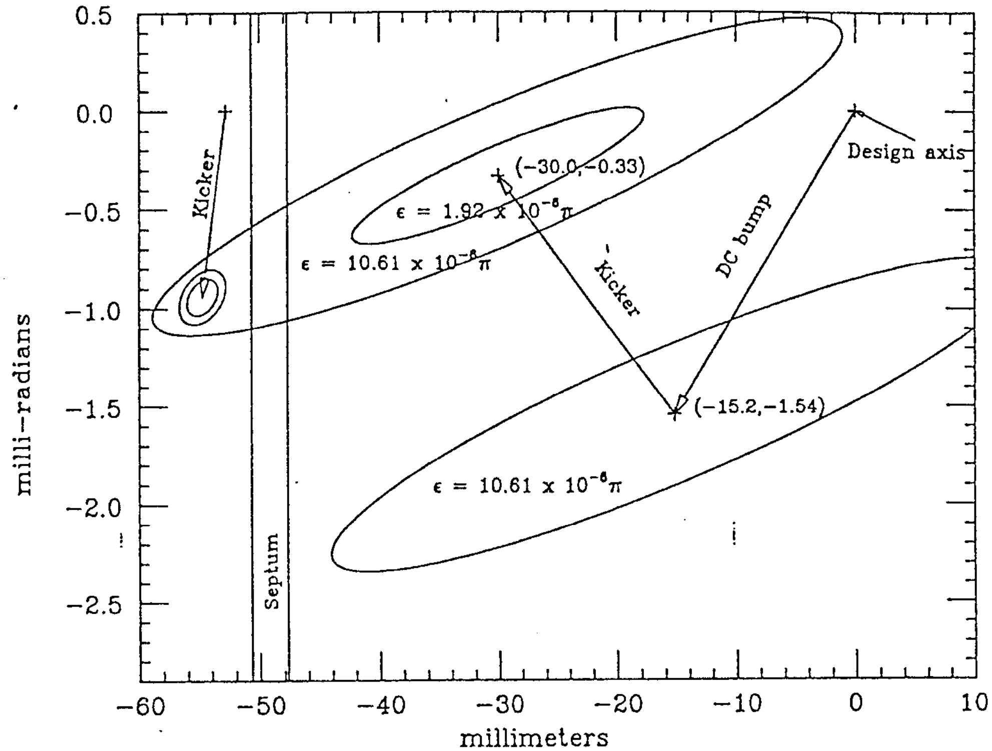

Horizontal phase space at exit of kicker magnet K2, showing injection for colliding beams.

Figure 10: 8 GeV NPI beam with single 0.5 mil B11 window

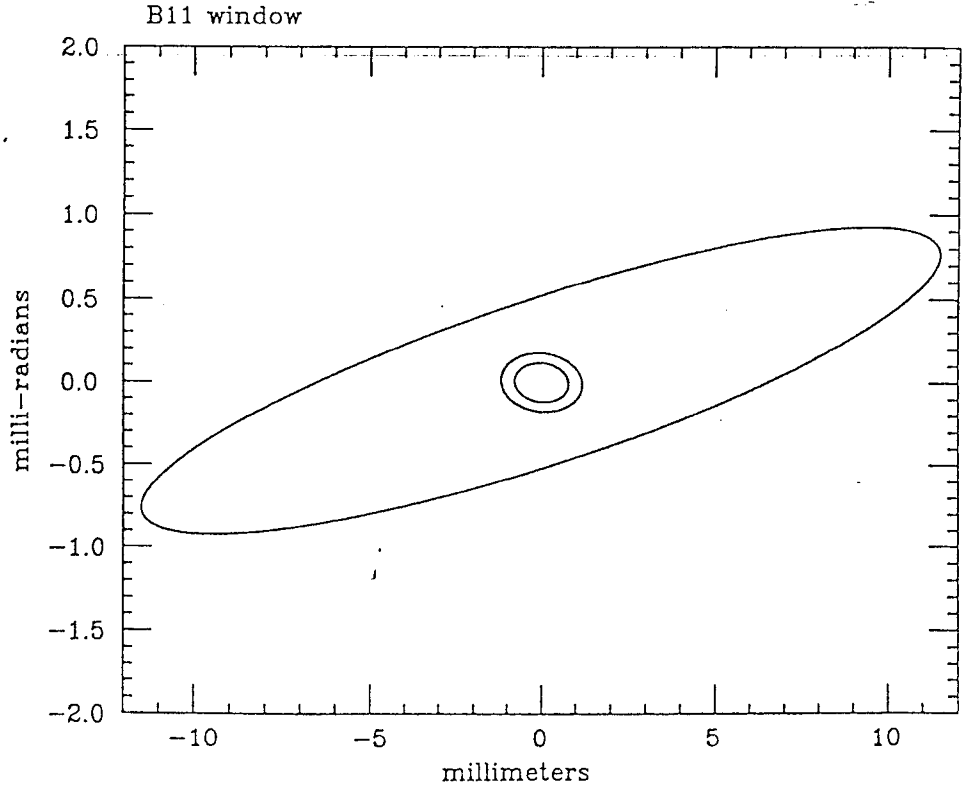

Vertical phase space at exit of kicker magnet K2, showing injection for colliding beams.

Figure 11: 8 GeV NPI beam with detector windows
and single 0.5 mil B11 window

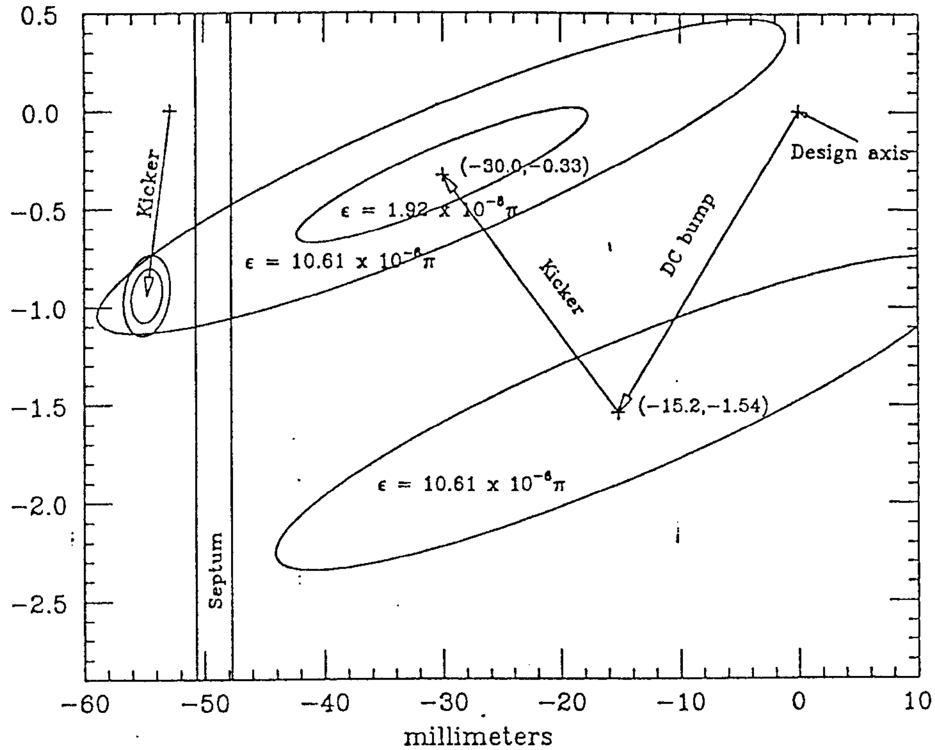

Horizontal phase space at exit of
kicker magnet K2, showing injection
for colliding beams.

Figure 12: 8 GeV NPI beam with detector windows
and single 0.5 mil B11 window

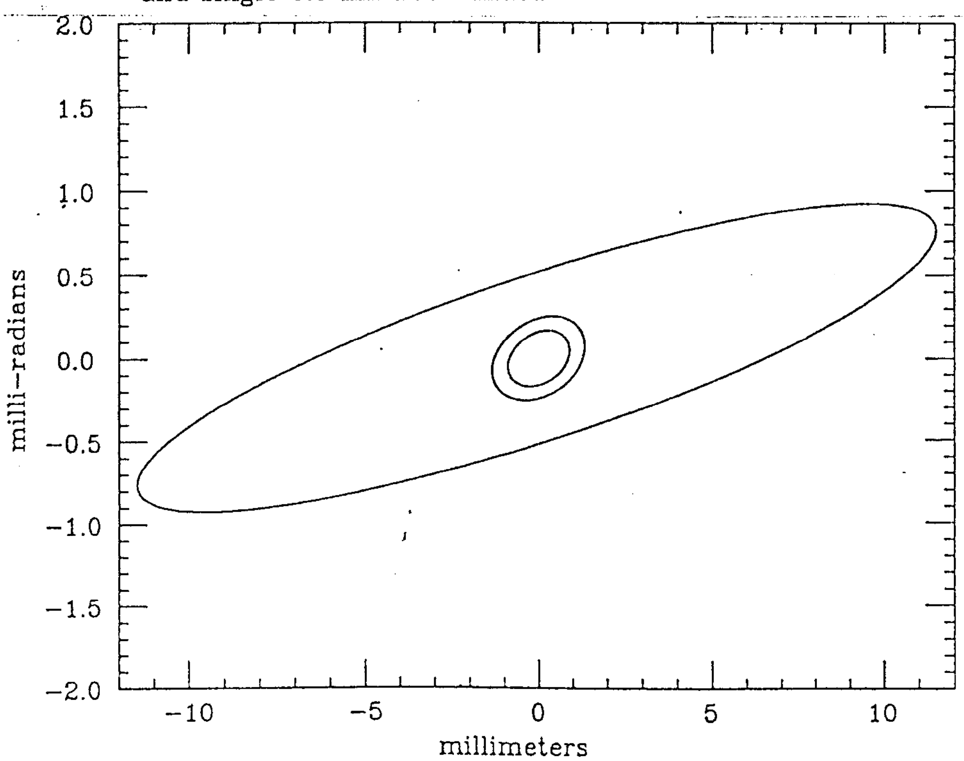

Vertical phase space at exit of
kicker magnet K2, showing injection
for colliding beams.

Figure 13: 8 GeV NPI beam with 4 B11 windows

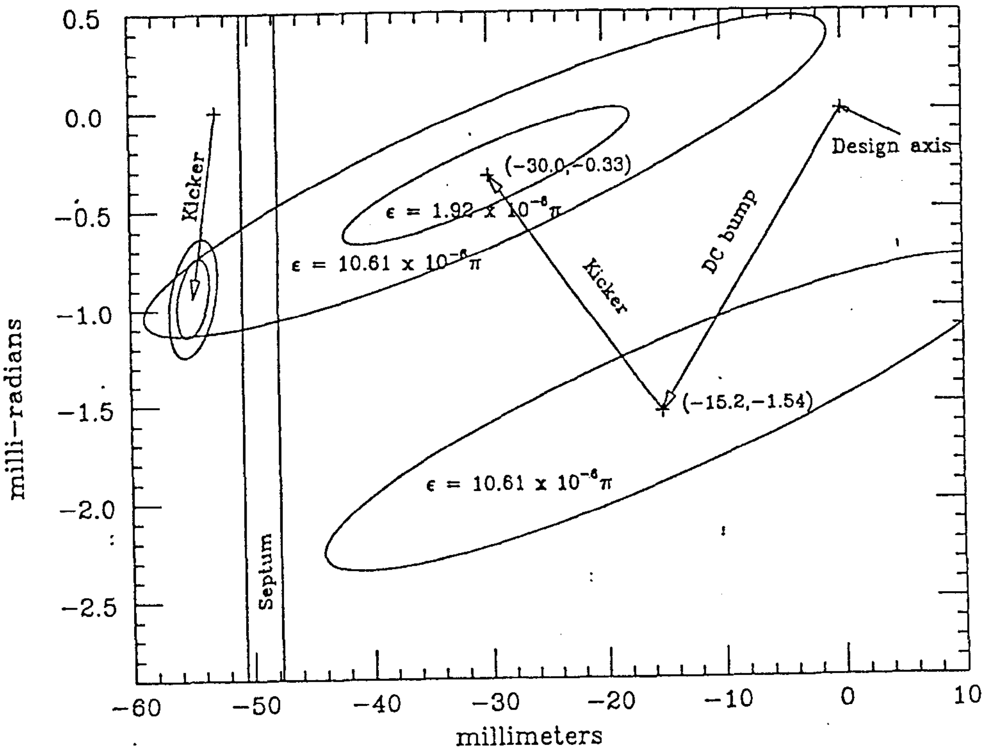

Horizontal phase space at exit of kicker magnet K2, showing injection for colliding beams.

Figure 14: 8 GeV NPI beam with 4 B11 windows

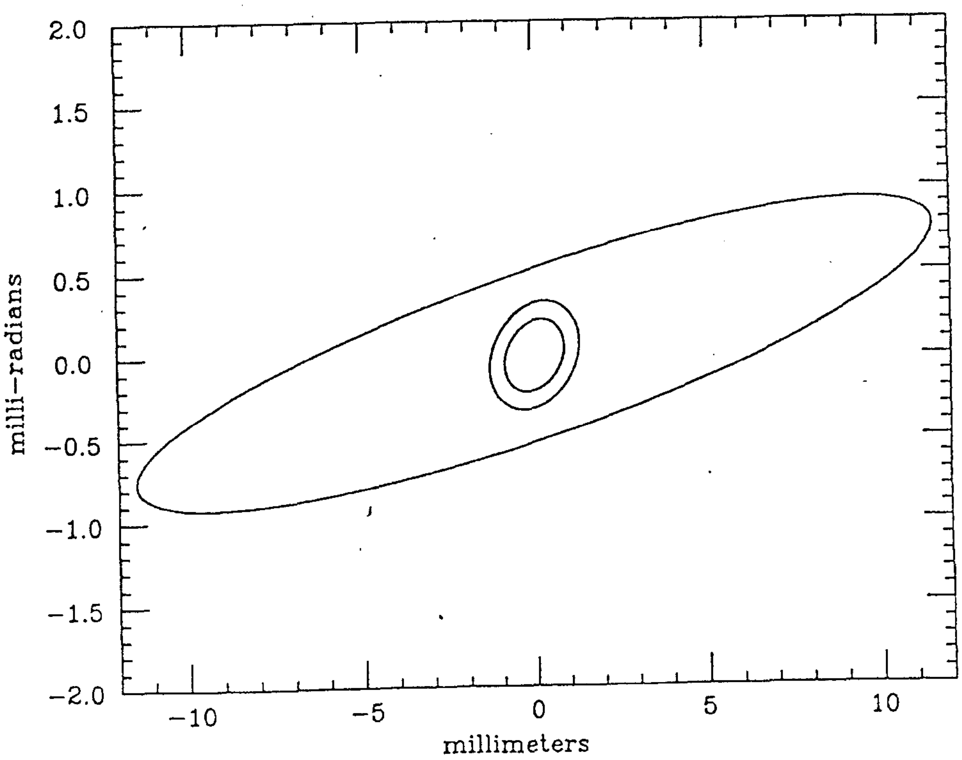

Vertical phase space at exit of kicker magnet K2, showing injection for colliding beams.

Figure 15: 13.5 GeV beam with former PEP emittancE of 0.0075 mm–mrad

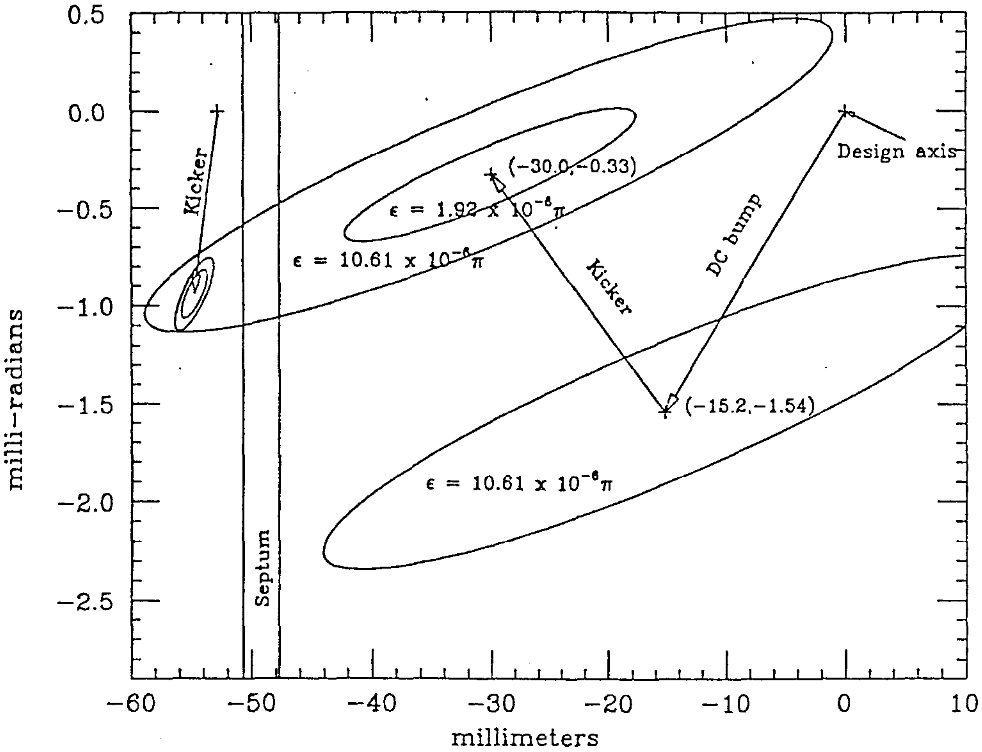

Horizontal phase space at exit of kicker magnet K2, showing injection for colliding beams.

Figure 16: 13.5 GeV beam with former PEP emittance of 0.0075 mm–mrad

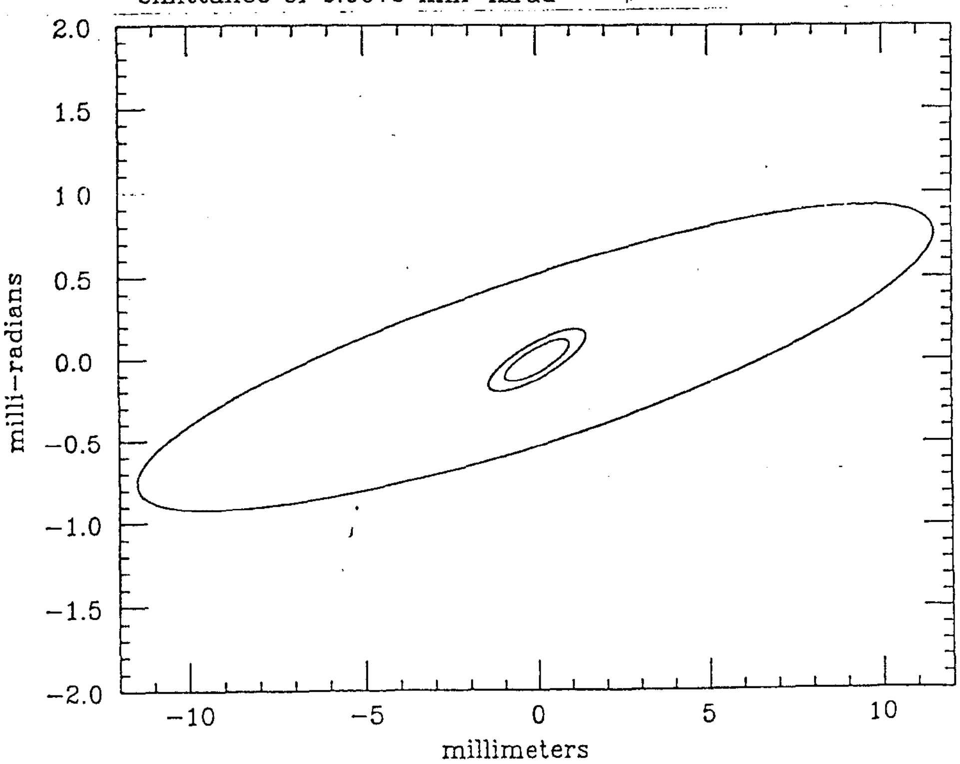

Vertical phase space at exit of kicker magnet K2, showing injection for colliding beams.

Figure 17

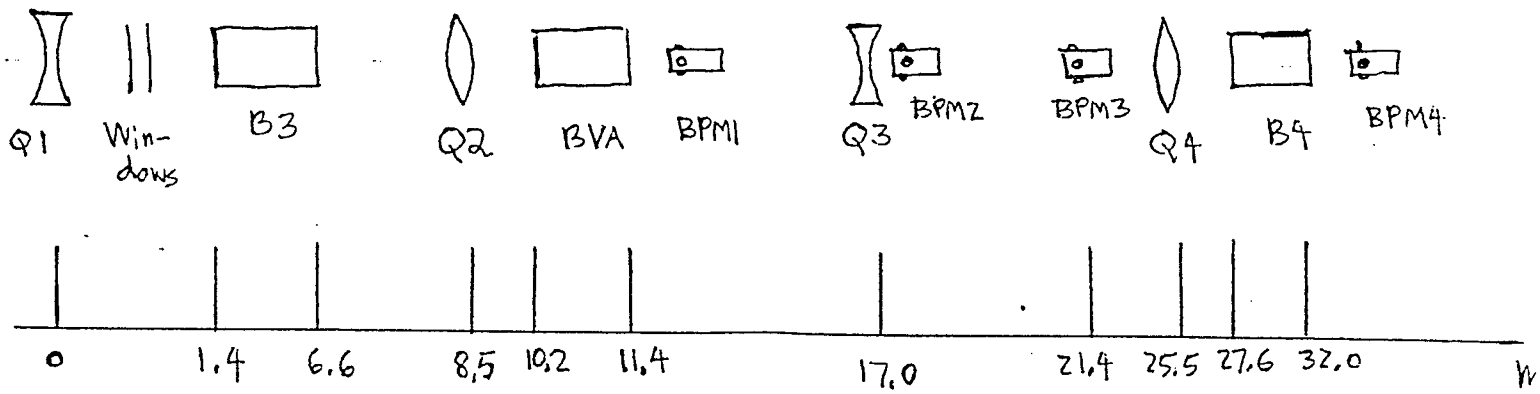

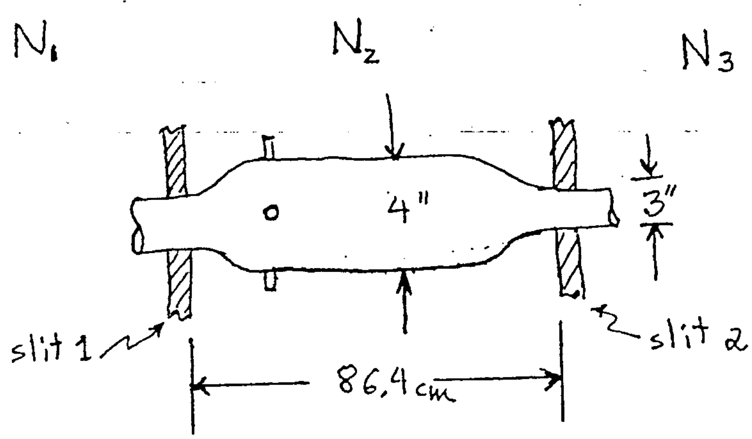

N_1 = number of rays upstream of slit 1.

N_2 = number of rays between slits 1 and 2.

N_3 = number of rays downstream of slit 2.

Figure 18 Scatter Plot of x vs. y at BPM 1

TWO DIMENSIONAL PLOT OF X VS Y

-10.000 0.000 10.000 TOTALS

y →, x ↓

		TOTALS
-60.000 TO -59.000 I		I 0
-59.000 TO -58.000 I		I 0
-58.000 TO -57.000 I		I 0
-57.000 TO -56.000 I		I 0
-56.000 TO -55.000 I		I 0
-55.000 TO -54.000 I		I 0
-54.000 TO -53.000 I		I 0
-53.000 TO -52.000 I		I 0
-52.000 TO -51.000 I		I 0
-51.000 TO -50.000 I		I 0
-50.000 TO -49.000 I		I 0
-49.000 TO -48.000 I		I 0
-48.000 TO -47.000 I		I 0
-47.000 TO -46.000 I		I 0
-46.000 TO -45.000 I		I 0
-45.000 TO -44.000 I		I 0
-44.000 TO -43.000 I		I 0
-43.000 TO -42.000 I		I 0
-42.000 TO -41.000 I		I 0
-41.000 TO -40.000 I		I 0
-40.000 TO -39.000 I		I 0
-39.000 TO -38.000 I	1	I 1
-38.000 TO -37.000 I	1	I 1
-37.000 TO -36.000 I	13	I 4
-36.000 TO -35.000 I	14	I 5
-35.000 TO -34.000 I	33	I 6
-34.000 TO -33.000 I	88	I 16
-33.000 TO -32.000 I	1MB1	I 35
-32.000 TO -31.000 I	6Z9	I 50
-31.000 TO -30.000 I	JY71	I 61
-30.000 TO -29.000 I	8Y9	I 48
-29.000 TO -28.000 I	2M$9	I 71
-28.000 TO -27.000 I	1NSD	I 80
-27.000 TO -26.000 I	3K$B1	I 72
-26.000 TO -25.000 I	3G$B	I 67
-25.000 TO -24.000 I	1WZ8	I 76
-24.000 TO -23.000 I	5H$8	I 79
-23.000 TO -22.000 I	3M$7	I 80
-22.000 TO -21.000 I	Q$9	I 74
-21.000 TO -20.000 I	3T$4	I 87
-20.000 TO -19.000 I	1KYB	I 66
-19.000 TO -18.000 I	5W$9	I 83
-18.000 TO -17.000 I	3U$9	I 91
-17.000 TO -16.000 I	2M$5	I 70
-16.000 TO -15.000 I	1TSC	I 89
-15.000 TO -14.000 I	2S$A	I 90
-14.000 TO -13.000 I	7Z$8	I 91
-13.000 TO -12.000 I	2W$6	I 82
-12.000 TO -11.000 I	2UZ7	I 74
-11.000 TO -10.000 I	5Z$5	I 86
-10.000 TO -9.000 I	4$$4	I 82
-9.000 TO -8.000 I	5Z$4	I 91
-8.000 TO -7.000 I	16YY7	I 79
-7.000 TO -6.000 I	7S$7	I 78
-6.000 TO -5.000 I	3$Y1	I 81
-5.000 TO -4.000 I	3$$91	I 98
-4.000 TO -3.000 I	8$U7	I 84
-3.000 TO -2.000 I	11$$4	I 83
-2.000 TO -1.000 I	62X8	I 82
-1.000 TO 0.000 I	4Z$4	I 81
0.000 TO 1.000 I	4$S6	I 89
1.000 TO 2.000 I	12$$3	I 97
2.000 TO 3.000 I	3$S	I 89
3.000 TO 4.000 I	3$Q1	I 72
4.000 TO 5.000 I	17$S6	I 99
5.000 TO 6.000 I	2$U2	I 73
6.000 TO 7.000 I	5Q$4	I 74
7.000 TO 8.000 I	C$V5	I 87
8.000 TO 9.000 I	4$X3	I 78
9.000 TO 10.000 I	CU$2	I 81
10.000 TO 11.000 I	4$R7	I 77
11.000 TO 12.000 I	4$V5	I 82
12.000 TO 13.000 I	5Z$	I 76
13.000 TO 14.000 I	4$R5	I 75
14.000 TO 15.000 I	5$$3	I 95
15.000 TO 16.000 I	16$V2	I 79
16.000 TO 17.000 I	5$Q1	I 72
17.000 TO 18.000 I	6$Q1	I 71
18.000 TO 19.000 I	BZQ1	I 73
19.000 TO 20.000 I	3$V5	I 77
20.000 TO 21.000 I	7$L3	I 75
21.000 TO 22.000 I	8$N1	I 69
22.000 TO 23.000 I	7$M3	I 69
23.000 TO 24.000 I	BZQ4	I 76
24.000 TO 25.000 I	A$J1	I 66
25.000 TO 26.000 I	6$K2	I 67
26.000 TO 27.000 I	9$M2	I 72
27.000 TO 28.000 I	1H$J	I 75
28.000 TO 29.000 I	16UE1	I 52
29.000 TO 30.000 I	5N8	I 36
30.000 TO 31.000 I	BL3	I 35
31.000 TO 32.000 I	1794	I 21
32.000 TO 33.000 I	772	I 16
33.000 TO 34.000 I	231	I 6
34.000 TO 35.000 I	1	I 1
35.000 TO 36.000 I	2	I 2
36.000 TO 37.000 I		I 0
37.000 TO 38.000 I		I 0
38.000 TO 39.000 I		I 0
39.000 TO 40.000 I		I 0
40.000 TO 41.000 I		I 0
41.000 TO 42.000 I		I 0
42.000 TO 43.000 I		I 0
43.000 TO 44.000 I		I 0
44.000 TO 45.000 I		I 0
45.000 TO 46.000 I		I 0
46.000 TO 47.000 I		I 0
47.000 TO 48.000 I		I 0
48.000 TO 49.000 I		I 0
49.000 TO 50.000 I		I 0
50.000 TO 51.000 I		I 0
51.000 TO 52.000 I		I 0
52.000 TO 53.000 I		I 0
53.000 TO 54.000 I		I 0
54.000 TO 55.000 I		I 0
55.000 TO 56.000 I		I 0
56.000 TO 57.000 I		I 0
57.000 TO 58.000 I		I 0
58.000 TO 59.000 I		I 0
59.000 TO 60.000 I		I 0

22
3013
1865

TOTALS I 00000008942140000000 I 4928

TOTAL NUMBER OF ENTRIES = 4928 INCLUD

Figure 19 Scatter plot of x vs. y at BPM 3

TWO DIMENSIONAL PLOT OF X VS Y

X	-10.000 0.000 10.000	TOTALS
-60.000 TO -59.000 I	I	0
-59.000 TO -58.000 I	I	0
-58.000 TO -57.000 I	I	0
-57.000 TO -56.000 I	I	0
-56.000 TO -55.000 I	I	0
-55.000 TO -54.000 I	I	0
-54.000 TO -53.000 I	I	0
-53.000 TO -52.000 I	I	0
-52.000 TO -51.000 I	I	0
-51.000 TO -50.000 I	I	0
-50.000 TO -49.000 I	I	0
-49.000 TO -48.000 I	I	0
-48.000 TO -47.000 I	I	0
-47.000 TO -46.000 I	1 I	1
-46.000 TO -45.000 I	263 I	11
-45.000 TO -44.000 I	2362 I	13
-44.000 TO -43.000 I	19C3 I	25
-43.000 TO -42.000 I	4FI3 I	40
-42.000 TO -41.000 I	12CC9 I	36
-41.000 TO -40.000 I	3FC2 I	32
-40.000 TO -39.000 I	12FG3 I	37
-39.000 TO -38.000 I	4HG I	37
-38.000 TO -37.000 I	[illegible] I	29
-37.000 TO -36.000 I	5EH1 I	37
-36.000 TO -35.000 I	3HF2 I	37
-35.000 TO -34.000 I	6HJ2 I	44
-34.000 TO -33.000 I	25DD1 I	34
-33.000 TO -32.000 I	4FB1 I	31
-32.000 TO -31.000 I	7F8 I	30
-31.000 TO -30.000 I	16K91 I	37
-30.000 TO -29.000 I	DM91 I	45
-29.000 TO -28.000 I	9J91 I	38
-28.000 TO -27.000 I	7GB1 I	35
-27.000 TO -26.000 I	17E42 I	28
-26.000 TO -25.000 I	BC82 I	33
-25.000 TO -24.000 I	1BF52 I	34
-24.000 TO -23.000 I	1BGC2 I	42
-23.000 TO -22.000 I	14A81 I	24
-22.000 TO -21.000 I	AK91 I	40
-21.000 TO -20.000 I	5D21 I	21
-20.000 TO -19.000 I	27OA I	43
-19.000 TO -18.000 I	25B7 I	25
-18.000 TO -17.000 I	CL7 I	40
-17.000 TO -16.000 I	CI7 I	37
-16.000 TO -15.000 I	1AN8 I	42
-15.000 TO -14.000 I	37F6 I	31
-14.000 TO -13.000 I	3EK3 I	40
-13.000 TO -12.000 I	2DM31 I	41
-12.000 TO -11.000 I	2DC21 I	30
-11.000 TO -10.000 I	1IP41 I	49
-10.000 TO -9.000 I	11JH5 I	43
-9.000 TO -8.000 I	2KM6 I	50
-8.000 TO -7.000 I	3JB41 I	38
-7.000 TO -6.000 I	11GH5 I	40
-6.000 TO -5.000 I	2HG2 I	37
-5.000 TO -4.000 I	ED6 I	33
-4.000 TO -3.000 I	5FI2 I	40
-3.000 TO -2.000 I	48A1 I	23
-2.000 TO -1.000 I	5CQ21 I	46
-1.000 TO 0.000 I	24FK3 I	44
0.000 TO 1.000 I	6F72 I	30
1.000 TO 2.000 I	3JM3 I	47
2.000 TO 3.000 I	4IG2 I	40
3.000 TO 4.000 I	2BG1 I	36
4.000 TO 5.000 I	5B53 I	24
5.000 TO 6.000 I	4LH2 I	44
6.000 TO 7.000 I	5N92 I	39
7.000 TO 8.000 I	1FF4 I	35
8.000 TO 9.000 I	4JA3 I	36
9.000 TO 10.000 I	7G91 I	33
10.000 TO 11.000 I	4FA1 I	30
11.000 TO 12.000 I	4FE I	33
12.000 TO 13.000 I	3LB2 I	37
13.000 TO 14.000 I	17DE2 I	37
14.000 TO 15.000 I	15JB2 I	38
15.000 TO 16.000 I	6T8 I	43
16.000 TO 17.000 I	5BB2 I	35
17.000 TO 18.000 I	13DA I	27
18.000 TO 19.000 I	29IC2 I	43
19.000 TO 20.000 I	9DC1 I	35
20.000 TO 21.000 I	8J8 I	35
21.000 TO 22.000 I	5F6 I	26
22.000 TO 23.000 I	7H91 I	34
23.000 TO 24.000 I	8061 I	39
24.000 TO 25.000 I	6E7 I	27
25.000 TO 26.000 I	1CJ7 I	39
26.000 TO 27.000 I	2BO91 I	47
27.000 TO 28.000 I	15A61 I	23
28.000 TO 29.000 I	GE61 I	37
29.000 TO 30.000 I	2GB3 I	32
30.000 TO 31.000 I	1AG51 I	33
31.000 TO 32.000 I	FK3 I	38
32.000 TO 33.000 I	1CC8 I	33
33.000 TO 34.000 I	2FL2 I	40
34.000 TO 35.000 I	2FJ3 I	39
35.000 TO 36.000 I	DK5 I	38
36.000 TO 37.000 I	9J7 I	35
37.000 TO 38.000 I	[illegible] I	27
38.000 TO 39.000 I	AG4 I	30
39.000 TO 40.000 I	1BK1 I	33
40.000 TO 41.000 I	2EG61 I	39
41.000 TO 42.000 I	38B I	22
42.000 TO 43.000 I	1BB1 I	24
43.000 TO 44.000 I	1C61 I	20
44.000 TO 45.000 I	4C6 I	22
45.000 TO 46.000 I	58 I	13
46.000 TO 47.000 I	122 I	5
47.000 TO 48.000 I	I	0
48.000 TO 49.000 I	1 I	1
49.000 TO 50.000 I	I	0
50.000 TO 51.000 I	I	0
51.000 TO 52.000 I	I	0
52.000 TO 53.000 I	I	0
53.000 TO 54.000 I	I	0
54.000 TO 55.000 I	I	0
55.000 TO 56.000 I	I	0
56.000 TO 57.000 I	I	0
57.000 TO 58.000 I	I	0
58.000 TO 59.000 I	I	0
59.000 TO 60.000 I	I	0
I	11 I	
I	4104 I	
I	335815 I	
TOTALS I	00000009314630000000 I	3176

TOTAL NUMBER OF ENTRIES = 3176 INCLU

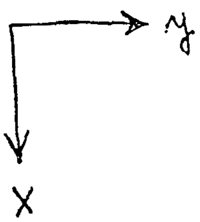

```
TWO DIMENSIONAL PLOT OF    Y VS    X

                        -60.000     -0.000     60.000 TOTALS
                        I**----*----*----*----**I--------
-10.000 TO  -9.000 I                        I       0
 -9.000 TO  -8.000 I                        I       0
 -8.000 TO  -7.000 I                        I       0
 -7.000 TO  -6.000 I                        I       0
 -6.000 TO  -5.000 I                        I       0
 -5.000 TO  -4.000 I          1             I       1
 -4.000 TO  -3.000 I        2  66           I      14
 -3.000 TO  -2.000 I     1127D6KRQG         I     119
 -2.000 TO  -1.000 I     1GX$$$$$$N         I     542
 -1.000 TO   0.000 I     J$$$$$$$$M         I     933
  0.000 TO   1.000 I     $$$$$$$$$6         I     914
  1.000 TO   2.000 I     T$$$$$$GI1         I     521
  2.000 TO   3.000 I     B$KGE752           I     116
  3.000 TO   4.000 I     1771               I      16
  4.000 TO   5.000 I                        I       0
  5.000 TO   6.000 I                        I       0
  6.000 TO   7.000 I                        I       0
  7.000 TO   8.000 I                        I       0
  8.000 TO   9.000 I                        I       0
  9.000 TO  10.000 I                        I       0
                   I**----*----*----*----**I--------
                   I                        I
                   I                        I
                   I       333433333        I
                   I       976819756 6      I
            TOTALS I 00000015001786800000  I    3176

       TOTAL NUMBER OF ENTRIES =        3176 INCLUDING UND
```

Figure **20** X vs. y at BPM2

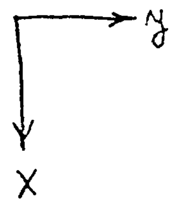


```
TWO DIMENSIONAL PLOT OF    Y VS    X

                        -60.000     -0.000     60.000 TOTALS
                        I**----*----*----*----**I--------
-10.000 TO  -9.000 I                        I       0
 -9.000 TO  -8.000 I                        I       0
 -8.000 TO  -7.000 I                        I       0
 -7.000 TO  -6.000 I                        I       0
 -6.000 TO  -5.000 I                        I       0
 -5.000 TO  -4.000 I                        I       0
 -4.000 TO  -3.000 I                        I       0
 -3.000 TO  -2.000 I                        I       0
 -2.000 TO  -1.000 I                        I       0
 -1.000 TO   0.000 I         U$$$$          I     639
  0.000 TO   1.000 I         $$$$B          I     648
  1.000 TO   2.000 I                        I       0
  2.000 TO   3.000 I                        I       0
  3.000 TO   4.000 I                        I       0
  4.000 TO   5.000 I                        I       0
  5.000 TO   6.000 I                        I       0
  6.000 TO   7.000 I                        I       0
  7.000 TO   8.000 I                        I       0
  8.000 TO   9.000 I                        I       0
  9.000 TO  10.000 I                        I       0
                   I**----*----*----*----**I--------
                   I                        I
                   I                        I
                   I          3222          I
                   I         807967         I
            TOTALS I 0000000474110000000 0 I    1287

       TOTAL NUMBER OF ENTRIES =        1287 INCLUDII
```

Figure **21** x vs. y at BPM4